Assessing the Impact of Urban Morphology on BIPV Potential in High-density Urban Area A Case Study in Shanghai

Li, Xinyu; Shi, Jie; Guo, Yucheng; Lin, Sixing; Niu, Xinman; Yang, Hui; Peng, Zhikai; Su, Lingqi

Publication date
2025

Document Version
Final published version

Published in
6th International Conference on Building Energy and Environment

Citation (APA)
Li, X., Shi, J., Guo, Y., Lin, S., Niu, X., Yang, H., Peng, Z., & Su, L. (2025). Assessing the Impact of Urban Morphology on BIPV Potential in High-density Urban Area: A Case Study in Shanghai. In *6th International Conference on Building Energy and Environment* COBEE.

6th International Conference on Building Energy and Environment
Eindhoven University of Technology, The Netherlands
6 - 10 July 2025

Assessing the Impact of Urban Morphology on BIPV Potential in High-density Urban Area: A Case Study in Shanghai

Xinyu Li [1], Jie Shi [1, *], Yucheng Guo [2,*], Sixing Lin [1], Xinman Niu [1], Hui Yang [1], Zhikai Peng [3], Lingqi Su [1, *]

[1] *Sino-German College of Applied Sciences, Tongji University, Shanghai, China, shijie@tongji.edu.cn; lingqi_su@tongji.edu.cn*

[2] *College of Architecture and Urban Planning, Tongji University, Shanghai, China, 2230059@tongji.edu.cn*

[3] *Delft University of Technology, Delft, Netherlands, z.p.peng@tudelft.nl*

SUMMARY

The building sector is a major contributor to global carbon emissions and energy consumption. A promising solution to mitigate this impact is the utilization of renewable energy, especially solar energy. However, in a high-density built environment, the application of photovoltaic (PV), especially on the building facades, is often hindered by shading from surrounding structures. To optimize solar energy use in urban area, it is important to understand the influence of key urban morphological parameters on solar energy utilization in densely built environment. This study aims to explore the relationship between urban morphology and building-integrated photovoltaic (BIPV) performance with a typological approach, while ensuring life cycle economic and environmental benefits. The findings are expected to inform design and planning strategies for effectively integrating solar energy into urban environments, thereby promoting more sustainable and energy-efficient cities and supporting long-term carbon neutrality objectives.

Keywords: High-density Urban Morphology, Solar Potential, Block Prototypes, Life Cycle Assessment

1. INTRODUCTION

1.1 Background

As one of the largest contributors to global energy consumption and greenhouse gas emission, cities should play a leading role in the process of energy transition. Thus, Solar energy is now widely used in built environments. Building-integrated photovoltaic (BIPV) integrates photovoltaic (PV) modules into building structures, providing the benefits of both clean energy production and enhanced building performance. However, the widespread application of BIPV faces several challenges. Besides economic barriers, a significant issue lies in the inflexibility of implementation, since the positioning of PV modules is often fixed during the construction phase. In the implementation of BIPV in high-density urban environments, the drawback of fixed-position installation of PV modules is further aggravated, where shading from surrounding structures can significantly decrease the PV performance. Therefore, meticulous planning and evaluation are crucial for the successful deployment and promotion of BIPV systems.

To provide a theoretical foundation for the planning of BIPV, this paper aims to investigate the impact of urban morphology on the potential of BIPV. Focusing on Shanghai as a representative high-density metropolis, this study explored the influence of key urban morphology on the BIPV energy potential at meso scale with the prototypes identified through clustering algorithm. The

findings of this study aim to offer valuable insights for optimizing BIPV integration in urban planning, thereby supporting the development of more sustainable and energy-efficient cities.

1.2 Literature Review

Strategic urban morphology planning has been recognized as a critical factor in maximizing solar energy utilization (Amado et al., 2012). Recent studies have adopted an established methodology that integrates quantitative urban morphology analysis with prototype selection, systematically examining parameter variations and their combinatorial effects on solar performance (Schirmer et al., 2016). One crucial step in this research lies in the identification of appropriate morphological parameters, which directly determines the representativeness of extracted urban block prototypes. The definitions of common parameters and their related literature can be found in Table 1.

Table 1. Morphological parameters commonly used in studies related to solar potential

Parameter	Description	Related Literature
Density / Building Coverage Ratio	Building Footprint Area / Site Area	Basic parameters adopted for the most research
Floor Area Ratio / Plot Ratio	Building Floor Area / Site Area	
Average Building Floor	Building Floor Area / Building Footprint Area	
Average Building Height	Average Building Height × Floor Height	
Sky View Factor	Upper hemisphere visible sky percentage	(Liu et al., 2023) (Poon et al., 2020)
Orientation	Orientation of the main façade of the building	(Mahaya et al., 2022) (Yang et al., 2024)
Open Space Ratio	1/ Floor Area Ratio – 1 / Average Building Floor	(Zhu et al., 2020) (Zhang et al., 2019)
The Form of Single Buildings	Single building form, including slab, tower, courtyard, etc.	(Tian er al., 2021)

The selection of research cases generally follows two approaches: analysis of existing urban configurations (Jareemit et al., 2025) or generation of sample library with different morphological parameters combination (Du et al., 2024). The difficulty with the former is how to select a representative prototype in a number of cases. Limitations of the latter approach in capturing real-world complexity have been shown in previous research. To over this bridge, this study employs real-world urban blocks in Shanghai as research prototypes with a clustering approach, the potential for solar potential will be compared to analyze the impact of morphology on it.

2. METHODOLOGY

This research consists of the following four stages, as shown in Figure 1.

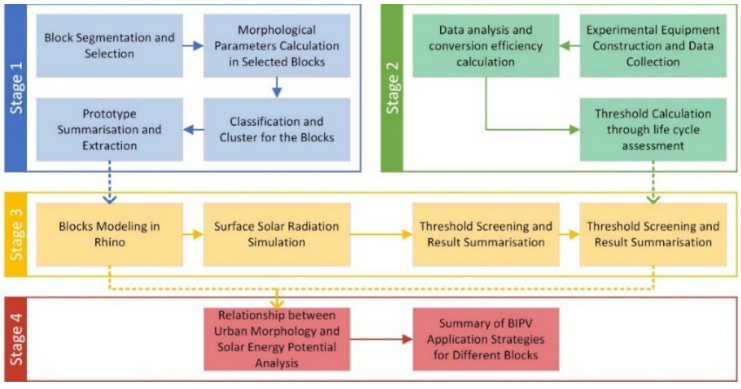

Figure 1. The Framework of this research

From the review of the related research in Section 1.2, 7 key parameters are selected for analyzing urban morphology, as shown in Table 2. Following the Chinese standard GB 50352-2019, we classified buildings into three categories: low-rise (1-3 floors), multi-rise (4-9 floors) and high-rise (≥10 floors). The prototype extraction process was implemented in two sequential stages. First, urban blocks were classified with density and average number of floors. Then, block types were clustered with the percentage of floor area of each building height category as the primary criterion.

Table 2. Selected morphological indicators

Parameter	Unit	Description
Block Area *A*	m^2	The site area of the research block
Building Footprint Area *F*	m^2	The footprint area of buildings in the research block
Building Floor Area *B*	m^2	The total building area in the research block
Density of Block *D*	-	F / B
Floor Area Ratio *FAR*	-	B / A
Average Building Floor N_{Floor}	-	B / F_t
Percentage of Floor Area of Different Type Building Height n_i	%	$S_{Building,\ i} / S_{Building}$

For BIPV performance evaluation, modules were constructed in building surface to evaluate conversion efficiency under real-world conditions. The experimental equipment is listed in Table 3. The radiation threshold is important for the selection of the usable building surfaces, ensuring both environmental and economic benefits. These benefits, noted as $R_{T,en}$ for environmental and $R_{T,ec}$ for economic benefits, can be calculated through Equations (1) and (2) , respectively. Table 4 details the values for each parameter in this study.

Table 3. Experiment devices

Equipment		Function	Sampling Rate
PV panels		Converting solar energy into electricity	-
Kipp & Zonen CMP11		Measuring solar radiation on the ground	-
Kipp & Zonen LOGBOX SE		Record the test data transmitted by CMA11	1 min
DAM3053DC		Measure the actual output power of the PV panel	1 min

$$R_{T,en} = \frac{\sum_{t=0}^{n} \frac{C_t}{(1+d)^t}}{\sum_{t=1}^{n} \frac{LCOE_t \times \eta_t}{(1+d)^t}} \tag{1}$$

$$R_{T,ec} = \frac{\sum_{t=0}^{n} EF_{PV,t}}{\sum_{t=1}^{n} EF_E \times \eta_t} \tag{2}$$

Table 4. Required Parameters for the performance evaluation

Parameter	Values
Life Cycle *n*	25a
Levelized Cost of Energy *LCOE*	0.737 RMB/kWh

Initial Investment C_0	3.0 RMB/W
Subsequent Investment C_t (t is from 1 to 25)	3% of the initial investment
Conversion Efficiency of PV η_t	Calculations based on experiment data. Annual degradation rate: 2.5%/a in the first year and 0.7 %/a thereafter
Discount Rate n	8%/a
Electricity Carbon Emission Factor EF_E	0.581kg/kWh
PV Carbon Emission Factor $EF_{PV,\,t}$	Only the carbon emission during production process is considered with the Report by Deloitte and Envision Group (Deloitee et al., 2024), 1.22 kgCO2/Wc

The block prototypes will be extracted through a clustering approach, then the geometry data of the selected cases are exported from ArcGIS and reconstructed into 3D models with Rhino. The simulation of the solar radiation on the building surfaces was performed with the Ladybug plug-in, enabling the identification of surfaces meeting the predefined application thresholds. Based on these results, a comparative analysis of BIPV application potential was conducted across different block types.

3. CASE STUDY

3.1 Block Prototype Extraction

Urban blocks serve as fundamental elements of urban fabric, enabling the analysis of building interactions and providing insights for larger-scale urban planning and design. This study adopts the three-tier living circle system as the scale of block extraction: 5-minute, 10-minute, and 15-minute walking distances. Given that a 5-minute walk for adults is approximately 400 meters, the block scales within the range of 400 m × 400 m to 1200 m × 1200 m, corresponding to an block area between 0.16 km^2 and 1.44 km^2. Block parcels were generated from urban data by first establishing road buffer zones. Road widths were set at 40 m, 30 m, 25 m, and 12 m, following Technical Standard of Highway Engineering (JTG B01-2014), resulting in 1,515 parcels. These parcels were further categorized into nine groups based on their density and their number of floors. Density classification was performed using the K-means algorithm (K=3), yielding three density clusters: low-density (< 0.18), middle-density (0.18–0.27), and high-density (> 0.27). The distribution of the nine block types is shown in Figure 2.

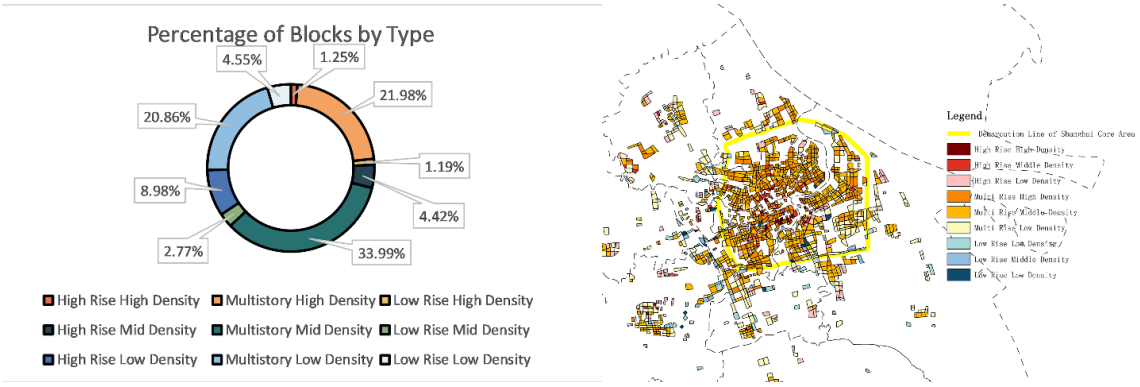

Figure 2. Percentage and Distribution of Blocks by Type (Urban Data Source: Baidu Map, OpenStreetMap)

High-rise high-density (HH), multi-rise high-density (MH), high-rise middle-density (HM) and

multi-rise middle-density (MM) blocks were identified as the dominant types in Shanghai center. Further analysis focused on the mixing ratios of high-rise, multi-rise, and low-rise floor areas within MH and MM blocks. The Affinity Propagation (AP) algorithm was employed to cluster blocks within each type. The MH blocks were further divided into four clusters: multi-rise dominated (MH-A), multi-rise low-rise hybrid (MH-B), multi-rise dominated multi-rise high-rise hybrid (MH-C), and high-rise dominated multi-rise high-rise hybrid (MH-D). Similarly, the MM blocks were classified into five clusters: multi-rise low-rise hybrid (MM-A), multi-rise dominated (MM-B), high-rise dominant mixed (MM-C), multi-rise intercourse mixed (MM-D) and high-rise multi-rise mixed (MM-E). The plot scales were further divided into three intervals of $0.16km^2$~$0.64km^2$ (small plot), $0.64km^2$~$1.00km^2$ (middle plot), and $1.00km^2$~$1.44km^2$ (huge plot).

Table 5. Prototypes used for research

Type	Small Plot (SP)	Middle Plot (MP)	Huge Plot (HP)
High-rise High-density (HH)	√		
Middle-rise High-density A (MH-A)	√	√	√
Middle-rise High-density B (MH-B)	√	√	√
Middle-rise High-density C (MH-C)	√	√	√
Middle-rise High-density D (MH-D)	√	√	
High-rise Middle-density (HM)	√	√	
Middle-rise Middle-density A (MM-A)	√	√	√
Middle-rise Middle-density B (MM-B)	√	√	√
Middle-rise Middle-density C (MM-C)	√	√	√
Middle-rise Middle-density D (MM-D)	√	√	√
Middle-riseMiddle-density E (MM-E)	√	√	√

3.2 Radiation Threshold for BIPV Application

For the performance evaluation, the nominal conversion efficiency of PV panels was assumed to be 17.36% in this study. Our experimental results indicated an average conversion efficiency found of 16.61%. Based on the calculation method described in Section 2.2, the radiation threshold for PV application can be calculated as $404.5kWh/m^2$ because of the economic factors considering the PV feed-in subsidy. This threshold can be reduced to $392.14kWh/m^2$ if carbon quota trading was incorporated into the analysis. For environmental benefits the threshold value is 91.46 kWh/m^2 to meet PV application requirements. Consequently, the threshold of 400 kWh/m^2 for PV application was selected in this study.

3.3 Building Solar Radiation Potential Analysis

Solar radiation analysis was conducted using the Ladybug tool within the Grasshopper plugin. A computational framework was established, as shown in Figure 3, which determines the solar radiation on building surfaces and identifies the areas meeting the specified radiation threshold. Simulations were performed for both roofs and façades across 29 selected urban blocks in Shanghai. The results of these calculations are summarized in Table 6.

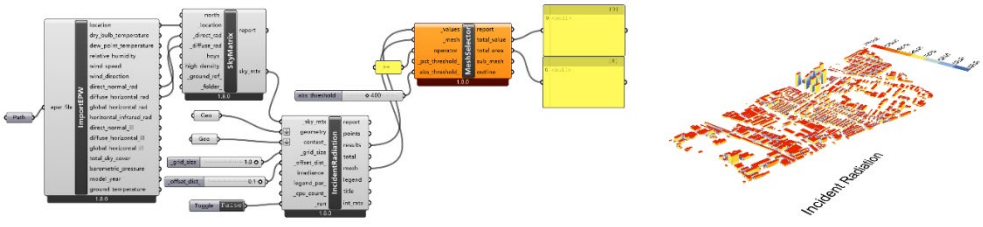

Figure 3. Grasshopper-LB-HB components for BIPV simulations and example of simulation results

Table 6-a. Simulation results (High Density)

Study Case	Radiation per unit area of the roof kWh/m^2	Radiation per unit area of the facade kWh/m^2	Radiation per unit area of all building surfaces kWh/m^2	Proportion of usable building surface area
HH SP	1039.14	563.75	730.40	28.62%
MH-A SP	1146.41	604.29	880.60	40.44%
MH-A MP	1159.95	658.94	988.84	49.38%
MH-A HP	1157.95	575.80	834.72	60.48%
MH-B SP	1166.04	571.43	904.53	59.91%
MH-B MP	1132.30	599.67	866.69	66.25%
MH-B HP	1152.92	603.12	819.99	60.29%
MH-C SP	1131.72	578.39	814.07	46.90%
MH-C MP	1134.20	591.54	844.84	44.60%
MH-C HP	1156.26	604.05	859.89	47.24%
MH-D SP	1091.25	598.10	812.55	49.94%
MH-D MP	1167.07	590.85	926.42	51.23%

Table 6-a. Simulation results (Middle Density)

Study Case	Radiation per unit area of the roof kWh/m^2	Radiation per unit area of the facade kWh/m^2	Radiation per unit area of all building surfaces kWh/m^2	Proportion of usable building surface area
HM SP	1190.55	588.22	808.59	38.68%
HM MP	1024.34	573.57	706.62	46.93%
MM-A SP	1172.92	652.21	937.50	58.63%
MM-A MP	1146.74	592.35	791.76	53.59%
MM-A HP	1117.65	597.60	804.57	42.96%
MM-B SP	1184.70	628.37	896.98	50.64%
MM-B MP	1162.40	590.76	810.57	42.10%
MM-B HP	1197.37	565.78	945.76	65.37%
MM-C SP	1088.40	583.27	796.80	37.23%
MM-C MP	1117.07	581.21	790.01	35.71%
MM-C HP	1150.87	620.31	866.88	32.65%
MM-D SP	1153.49	563.90	789.24	41.18%
MM-D MP	1163.77	601.10	877.67	46.39%
MM-D HP	1130.74	585.80	787.21	41.57%
MM-E SP	1141.93	609.69	836.52	46.45%
MM-E MP	1147.80	587.00	752.62	45.63%
MM-E HP	1127.02	606.94	826.61	36.56%

4. DISSCUSSION

These block types exhibit significant vertical development intensity, especially for MH-A MP, MM-B SP resulting in façade areas substantially larger than roof areas. This morphological feature highlights the considerable potential for façade-integrated BIPV applications. The analysis of BIPV potential can be categorized into two aspects: irradiation per unit area and the proportion of usable area, which determine the quality and quantity of BIPV deployment.

The solar energy potential of roofs is found to be relatively consistent across 29 study examples and less affected by morphological variations, with the irradiation levels exceeding 1000 kWh/m^2. In contrast, the solar potential of façades is significantly influenced by morphology. Despite the threshold of 400 kWh/m^2, the average radiation intensity on qualifying façade surfaces exceeded 550 kWh/m^2, ensuring both economic viability and substantial coverage of building surfaces. Meanwhile, building height emerged as a critical factor of the overall solar potential, as seen in both HH and HM cases ranking at the bottom in BIPV performance (Table 6-a, 6-b).

Among MH blocks, the MH-A type performed well across all three scales, while MH-B demonstrates the highest radiant intensity. MH-C exhibits optimal performance in compact plots, while MH-D demonstrates better performance only in medium plots. Within MM blocks, MM-B shows consistent suitability across multiple scales. These results suggest that multi-rise-dominated or multi-rise-low-rise hybrid configurations are most suitable for both MM and MH blocks.

In terms of the proportion of usable surfaces, HH blocks consistently showed the lowest values. Among MH blocks, MH-B has the highest proportion of usable surfaces, while MH-C has the lowest. Within MM blocks, MM-A and MM-B achieved the largest proportions of usable surfaces, with MM-D and MM-E demonstrating similar performance with over 40% of usable area. Conversely, MM-C shows the lowest proportion of usable area.

These results reveal that multi-rise-dominated or multi-rise and low-rise mixed-type blocks generally outperform high-rise blocks in solar energy potential within Shanghai's high-density urban context.This suggests that urban planners could prioritize mid-rise developments in area with high solar resources, while reserving high-rise typologies for areas where vertical density provides critical benefits. Such approach would balance the energy efficiency objectives with broader urban development goals.

5. CONCLUSION

This study investigated the impact of urban morphology on building-integrated photovoltaic (BIPV) potential in high-density urban environments, using Shanghai as a case study. With a clustering approach, urban blocks were classified into nine types, with four dominant types identified in the city's core: high-rise high-density (HH), multi-rise high-density (MH), high-rise medium-density (HM), and multi-rise medium-density (MM). These blocks were further subdivided into 29 clusters based on the plot scale and the mixing of various building height types. The solar radiation threshold was determined with a PV life cycle analysis framework. The solar radiation simulations were conducted for 29 selected block samples, and surfaces meeting the threshold were identified and analyzed. The results revealed significant variations in solar potential across different morphological block types, with multi-rise-dominated and multi-rise-low-rise hybrid configurations demonstrating the highest potential for BIPV applications. These insights shall provide valuable guidance for urban planners and policymakers aiming to integrate BIPV systems into high-density urban environments, ultimately supporting the development of more sustainable and energy-efficient cities.

However, this study has several limitations. First, the sample size was insufficient for rigorous quantitative analysis of the relationship between morphology parameters and solar energy

potential. Second, the abstraction process of quantifying the urban morphology was only limited to several parameters, which may not fully capture the complexity of morphology's influence on solar energy potential.

These limitations will be addressed in our future research, by incorporating interpretable machine learning methods based on the expanded sample size to enhance the robustness and generalizability of the findings and so that a quantitative relationship can be addressed for decision-making in the design and urban planning process. The external factors such as air pollution and season will be also considered in a more detailed experimental design to calculate the conversion efficiency to increase the credibility of the results. Furthermore, the spatial-temporal transportability of the results is also significant which determines the value of the application. Migration studies within and across climate zones will be further developed to confirm the validity of the method.

ACKNOWLEDGEMENTS

This work is supported by Student Innovation Training Program (No. X2024353), we would like to express our gratitude to this funding, also for the reviewers for their invaluable suggestions.

REFERENCES

Schirmer, P. M., & Axhausen, K. W. (2016). A multiscale classification of urban morphology. Journal of Transport and Land Use, 9(1), 101-130.

Amado, M., & Poggi, F. (2012). Towards Solar Urban Planning: A New Step for Better Energy Performance. Energy Procedia, 30, 1261-1273. https://doi.org/https://doi.org/10.1016/j.egypro.2012.11.139

Zhu, D., Song, D., Shi, J., Fang, J., & Zhou, Y. (2020). The Effect of Morphology on Solar Potential of High-Density Residential Area: A Case Study of Shanghai. Energies, 13(9). https://doi.org/10.3390/en13092215

Liu, K., Xu, X., Zhang, R., Kong, L., Wang, W., & Deng, W. (2023). Impact of urban form on building energy consumption and solar energy potential: A case study of residential blocks in Jianhu, China. Energy and Buildings, 280, 112727. https://doi.org/https://doi.org/10.1016/j.enbuild.2022.112727

Tian, J., & Xu, S. (2021). A morphology-based evaluation on block-scale solar potential for residential area in central China. Solar Energy, 221, 332-347. https://doi.org/https://doi.org/10.1016/j.solener.2021.02.049

Li, D., Cui, X., Shi, L., & Li, Y. (2024). An overview of the research on the correlation between solar energy utilization potential and spatial morphology. Results in Engineering, 24, 103444. https://doi.org/https://doi.org/10.1016/j.rineng.2024.103444

Poon, K. H., Kämpf, J. H., Tay, S. E. R., Wong, N. H., & Reindl, T. G. (2020). Parametric study of URBAN morphology on building solar energy potential in Singapore context. Urban Climate, 33, 100624. https://doi.org/https://doi.org/10.1016/j.uclim.2020.100624

Mahaya, C., Zemmouri, N., Benharra, H., & Elnokaly, A. (2022). Solar Access Assessment in Semi-Arid Urban Context: An Application Study for Ten Urban Forms of Existing Apartment Buildings Districts in Batna City, Algeria. Sustainable Cities and Society, 83, Article 103909. https://doi.org/10.1016/j.scs.2022.103909

Yang, C., Cai, S., & Gou, Z. (2024). Unlocking solar potential in high-latitude urban areas: A study of morphological indicators and zero energy potential of Glasgow. Solar Energy, 283, 113023. https://doi.org/https://doi.org/10.1016/j.solener.2024.113023

Zhang, J., Xu, L., Shabunko, V., Tay, S. E. R., Sun, H., Lau, S. S. Y., & Reindl, T. (2019). Impact of urban block typology on building solar potential and energy use efficiency in tropical high-density city. Applied Energy, 240, 513-533. https://doi.org/10.1016/j.apenergy.2019.02.033

Du, S., Kuang, X., Chen, J., Ye, Y., Li, P., & Shi, X. (2024). Development of an expanded local climate zone scheme to accommodate diversified urban morphological evolution: A case study of Shanghai, China. Urban Climate, 56, 102009. https://doi.org/https://doi.org/10.1016/j.uclim.2024.102009

Jareemit, D., Srivanit, M., Tanapant, S., & Limeechokchai, B. (2025). Role of urban morphology integrated building envelope materials in achieving zero emissions: A simulation-based study in complex-shaped urban blocks. Energy Reports, 13, 27-39. https://doi.org/https://doi.org/10.1016/j.egyr.2024.11.088

Deloitte, Envision Group (2024). Photovoltaic Modules - Carbon Footprint and Low Carbon Development Report. https://www2.deloitte.com/content/dam/Deloitte/cn/Documents/climate-sustainability/deloitte-cn-sustainability-photovoltaic-modules-report-zh-240425.pdf